

1 Duration and nature of the end-Cryogenian (Marinoan) glaciation

2 ¹Anthony R. Prave, ²Daniel J. Condon, ³Karl Heinz Hoffmann, ²Simon Tapster, and ⁴Anthony
3 **E. Fallick**

4 ¹*Department of Earth and Environmental Sciences, University of St Andrews, St Andrews, KY16*
5 *9AL, UK*

6 ²*NERC Isotope Geosciences Laboratory, British Geological Survey, Nottingham, NG12 5GG, UK*

7 ³*Geological Survey of Namibia, 1 Aviation Road, Windhoek, Namibia*

8 ⁴*Scottish Universities Environmental Research Centre, East Kilbride, G75 0QF, UK*

9

10 **ABSTRACT**

11 The end-Cryogenian glaciation (Marinoan) was Earth's last global glaciation yet its duration
12 and character remain uncertain. Here we report U-Pb zircon ages for two discrete ash beds within
13 glacial-marine deposits from widely separated localities of the Marinoan-equivalent Ghaub Formation
14 in Namibia: $639.29 \pm 0.26/0.31/0.75$ Ma and $635.21 \pm 0.59/0.61/0.92$ Ma. These findings, for the
15 first time, verify the key prediction of the Snowball Earth hypothesis for the Marinoan glaciation:
16 longevity, with a duration of $\geq 4.08 \pm 0.64$ Myr. They also show that glacial sedimentation,
17 erosion, and at least intermittent open-water conditions occurred 4 million years prior to termination
18 of the Marinoan glaciation and that the interval of non-glacial conditions between the two
19 Cryogenian glaciations was 20 Myr or less.

20 **INTRODUCTION**

21 The Cryogenian Period (*c.* 720 – 635 Ma) was marked by the two most severe glaciations in
22 Earth history (Hoffman et al., 1998; Fairchild and Kennedy, 2007), the older Sturtian and younger
23 Marinoan, and their association with unique lithofacies of cap carbonates (Kennedy et al., 2001;
24 Hoffman and Schrag, 2002; Hoffman et al., 2011), stable isotope fluctuations (carbon, oxygen,
25 boron, calcium; Halverson et al., 2005; Kasemann et al., 2005; Bao et al., 2008) and banded iron
26 formation are evidence for global-scale environmental changes with postulated links to ocean-

27 atmosphere oxygenation and biosphere evolution (Butterfield, 2009; Och and Sjiels-Zhou, 2012;
28 Sperling et al., 2013). Creation of a unified theory explaining those phenomena, however, has been
29 hampered by one key obstacle: a lack of temporal constraints. Recently, the Sturtian was shown to
30 have spanned an astonishing 56 Myr, from about 716 Ma to 660 Ma (Bowring et al., 2007;
31 Macdonald et al., 2010; Rooney et al., 2014; Rooney et al., 2015). In contrast, the duration of the
32 Marinoan is unresolved: it terminated at *c.* 635 Ma (Hoffmann et al. 2004; Calver et al., 2004;
33 Condon et al., 2005; Zhang et al., 2008) but its initiation can only be stated as being younger than
34 interglacial strata, which in Mongolia have been dated as *c.* 659 Ma (Rooney et al., 2014) and in
35 China as *c.* 655 Ma (Zhang et al., 2008). Here we report new dates for the Marinoan-equivalent
36 Ghaub Formation in Namibia that provide a basis for assessing the timing and nature of Earth's last
37 global glaciation.

38 **GEOLOGY: SAMPLES DW-1 AND NAV-00-2B**

39 The Nosib, Otavi and Mulden Groups comprise the Neoproterozoic sedimentary record of
40 the Congo craton in northern Namibia (Fig. 1). The Otavi Group (and correlative rocks in the
41 Swakop Group of the Outjo and Swakop Zones) is a 2-5 km thick carbonate platform-slope-basin
42 succession formed in the tropics along the margin of the Congo Craton. It is punctuated by two
43 Cryogenian glacial units (Hoffmann and Prave, 1996; Hofman and Halverson, 2008), the older
44 Chuos and the younger Ghaub formations and their respective cap carbonates, the Rasthof and
45 Keilberg formations. U-Pb zircon ages on igneous and volcanic units provide geochronological
46 constraints (see Fig. 1) that bracket deposition of the glacial-bearing strata in the Otavi Group to
47 between *c.* 756 Ma and 635 Ma.

48 One of the most informative exposures of the Ghaub Formation in northern Namibia is
49 along Fransfontein Ridge (Fig. 1). There, the Ghaub rocks vary in thickness from 1 to 600 m and
50 can be traced continuously for *c.* 70 km; they consist mostly of stratified and massive carbonate-
51 clast-rich diamictite, minor intervals of rippled and cross-stratified dolomitic grainstone, marl and
52 shale, and an upper unit, the 1 to 15 m thick Bethanis member (Hoffman and Halverson, 2008)

53 typified by cm- to dcm-thick stratified diamictite and grainstone-mudstone, all with abundant
54 variably sized dropstones. Detailed studies (Hoffman and Halverson, 2008; Domack and Hoffmann,
55 2011) of those lithofacies have interpreted them as a succession of moraine and glacimarine
56 sediments deposited along the margin of a repeatedly advancing and back-stepping ice-grounding
57 line (Domack and Hoffmann, 2011).

58 Along Fransfontein Ridge, the diamictite-dominated Ghaub Formation contains lenses,
59 generally a few metres thick, consisting of graded grainstone and laminated to massive calcareous-
60 dolomitic marl-shale with stringers of dropstones. At Duurwater (Fig. 2) one of these lenses about
61 15 m below the base of the Keilberg cap dolostone contains a prominent ash bed, sampled as DW-1
62 (Fig. 3). The DW-1 ash bed is 0.3 m thick, pale tan to pale yellow in colour, characterised by sharp
63 upper and lower contacts, displays a slight fining-upward grading, contains rare disseminated quartz
64 spar crystals and is overlain and underlain by IRD beds (Fig. 4A). These features indicate that this
65 bed is an air-fall tuff contemporaneous with deposition of the glacimarine sediments, hence its age
66 would also be the age of sedimentation for this part of the Ghaub Formation. Below the DW-1 ash
67 bed is 10-15m of massive diamictite and then a more than 100-m-thick succession of carbonate
68 rhythmite, breccia, laminated marl and shale with dispersed dropstones and isolated metre-scale and
69 larger blocks derived from pre-Ghaub formation units. These lithofacies fill a steep-sided incision
70 cut into the pre-Ghaub stratigraphy (Figs. 2, 3); in places along the Fransfontein outcrop belt as
71 much as 300 m of strata have been cut out along this surface.

72 Sample NAV-00-2B comes from an ash bed in the basinal equivalent of the Ghaub
73 Formation *c.* 30 m below the contact with the Keilberg cap dolostone at Navachab in central
74 Namibia (Fig. 3). This occurrence was reported by Hoffman et al. (2004) and readers are referred to
75 that paper for details.

76 **METHODS AND RESULTS**

77 All zircon dates in this study were obtained using established chemical abrasion (CA)
78 isotope dilution thermal ionisation mass spectrometry (ID-TIMS) methods at the NERC Isotope

79 Geoscience Laboratory of the British Geological Survey (Noble et al., 2015; see Data Repository
80 for details). U-Pb dates have been determined relative to the gravimetrically calibrated
81 EARTHTIME mixed U/Pb tracers (Condon et al., 2015; McLean et al., 2015) and ^{238}U and ^{235}U
82 decay constants (Jaffey et al., 1971; Mattinson, 2010).

83 Sample DW-1 yielded a population of zircons with a consistent morphology (aspect ratio ~ 2
84 and long axis typically 200 to 300 μm) and colour. Ten zircons were dated by CA-ID-TIMS; U-Pb
85 data for each analysis are concordant when the uncertainty in the ^{238}U and ^{235}U decay constants
86 (Mattinson, 2010) are considered (Fig. 4B; Data Repository Table 1). All analyses yield a weighted-
87 mean $^{207}\text{Pb}/^{206}\text{Pb}$ date of $639.1 \pm 1.7/1.8/5.0$ (n=10, MSWD=1.08). Of those, one analysis has
88 dispersion beyond that expected due to analytical scatter (see Data Repository) and is an obvious
89 outlier with a U-Pb date younger than the main population. Excepting this grain, the other nine
90 analyses yield a weighted mean $^{206}\text{Pb}/^{238}\text{U}$ date of $639.29 \pm 0.26/0.31/0.75$ Ma (95% confidence
91 interval, n=9, MSWD=2.6), which we interpret as the age of deposition.

92 Sample NAV-00-2B is an aliquot of the sample dated previously as 635.5 ± 1.2 Ma
93 (Hoffmann et al., 2004) at the Massachusetts Institute of Technology. Re-analysis of this sample
94 was done to capitalise on the use of CA for the effective elimination of Pb-loss (Mattinson, 2005)
95 and the EARTHTIME tracer and its comprehensive gravimetric calibration and uncertainty model
96 (Condon et al., 2015; McLean et al., 2015). The $^{206}\text{Pb}/^{238}\text{U}$ date for NAV-00-2B derived in this
97 study is $635.21 \pm 0.59/0.61/0.92$ Ma (95% confidence interval, n=5, MSWD=3.4; Fig. 4B, Data
98 Repository Table 2). This date is based upon a subset of the analyses (as explained in the Data
99 Repository) and, even given improved analytical precision and accuracy, is indistinguishable from
100 the date published in Hoffmann et al. (2004).

101 **DISCUSSION**

102 The $639.29 \pm 0.26/0.31/0.75$ Ma age for the DW-1 ash bed at Duurwater and the revised age
103 of $635.21 \pm 0.59/0.61/0.92$ Ma for the NAV-00-2B ash bed at Navachab now, for the first time,
104 confirm that the Marinoan glaciation was long-lived, lasting at least 4.08 ± 0.64 Myr. This verifies

105 the key prediction of the Snowball Earth hypothesis for a long duration glaciation. The revised age
106 for NAV-00-2B also refines and reconfirms that the timing of termination of the Marinoan
107 glaciation was synchronous worldwide (*i.e.* within error of the age data), occurring between 635.21
108 $\pm 0.59/0.61/0.92$ Ma and 635.2 ± 0.5 Ma, the age of an ash bed in the lower part of the cap
109 carbonate sequence in China (Condon et al., 2005); a conclusion reinforced by the U-Pb zircon age
110 of 636.41 ± 0.45 Ma for a volcanoclastic unit in the glacial-cap carbonate transition in Tasmania
111 (Calver et al., 2004).

112 Since the debut of the Snowball Earth hypothesis, debate has ensued regarding the extent of
113 land and sea ice during Cryogenian glaciations, the causes of repetitive patterns of inferred
114 proximal-distal and advance-retreat deposits, and the overall timing and duration of glacial
115 sedimentation (*e.g.* see discussion by Spence et al., 2016, and references therein). Further, the lack
116 of well-defined age models has led to an array of climate state and sedimentation scenarios, ranging
117 from surmising that the Marinoan rock record formed by glacial-interglacial-scale epochs (*e.g.*
118 Allen and Etienne, 2008; LeHeron et al., 2011) to interpretations of the bulk of that record as
119 having been deposited during a brief interval of time near to the end of the glacial state (*e.g.* Benn et
120 al., 2015). Although these interpretations are not necessarily mutually exclusive, assessing them
121 remains speculative because of the lack of constraints for the absolute timing of sedimentation. Our
122 new geochronological data provide a better temporal framework for understanding the Marinoan
123 glaciation. For example, the *c.* 639 Ma DW-1 ash bed occurring above a *c.* 100-m-thick glacimarine
124 succession shows that glacial erosion and sediment accumulation concurrent with at least
125 intermittent open-water conditions in the tropics existed more than 4 million years before the
126 ultimate meltback phase of the Marinoan ice sheets. This impacts on a range of issues regarding the
127 Marinoan climate state: it provides constraints and corroboration of models that yield results
128 consistent with such conditions, including predictions of plausible CO₂ levels permissive of
129 enabling ice-line migration and associated sedimentation in the tropics, as documented for the
130 Ghaub Formation (*e.g.* Domack and Hoffman, 2011), to considerations of low-latitude *refugia* and

131 the survival of eukaryotic organisms within the main phase of the Marinoan glaciation. Further,
132 given our new age that provides a minimum duration for the Marinoan glaciation and the *c.* 660 Ma
133 age for the end of the older Cryogenian glaciation (Sturtian), the intervening interglacial interval
134 and associated biogeochemical and isotopic events represent a timespan of 20 Myr or less (Fig. 4C).
135 Determining how and why this period of non-glacial conditions punctuated an otherwise apparently
136 consistently and largely ice-covered Earth poses an intriguing research question.

137

138 **CONCLUSION**

139 The $639.1 \pm 1.7/1.8/5.0$ Ma age obtained on an ash bed in glacial marine sediments of the
140 Marinoan-equivalent Ghaub Formation in northern Namibia combined with a refined age of 635.21
141 $\pm 0.59/0.61/0.92$ Ma for an ash bed in the basinal equivalent of the Ghaub Formation in central
142 Namibia confirm that the Marinoan glaciation was long-lived, at least 4 Myr in duration, and that
143 the preceding interval of non-glacial conditions was less than 20 Myr in duration. Our data also
144 confirm that the sedimentary archive of the Marinoan glaciation records glacial erosion-
145 sedimentation and at least intermittent open-water conditions as much as 4 million years prior to
146 terminal meltback at *c.* 635 Ma.

147

148 **ACKNOWLEDGMENTS**

149 This work was supported by NIGFSC grant IP XXXXXX.

150

151 **REFERENCES CITED**

152 Allen, P.A., and Etienne, J.L., 2008, Sedimentary challenge to Snowball Earth: *Nature Geosciences*,
153 v. 1, p. 817-825.

154 Bao, H., Lyons, J.R., and Zhou, C., 2008, Triple oxygen isotope evidence for elevated CO₂ levels
155 after a Neoproterozoic glaciation: *Nature*, v. 453, p. 504-506.

156 Benn, D.I., Le Hir, G., Bai, H., Donnadieu, Y., Dumas, C., Fleming, E.J., Hambrey, M.J.,
157 McMillan, E.A., Petronis, M.S., Ramstein, G., Stevenson, C.T.E., Wynn, P.M., Fairchild, I.J.,
158 2015, Orbitally forced ice sheet fluctuations during the Marinoan Snowball Earth glaciation:
159 Nature Geoscience, v. 8, p. 704-707.

160 Bowring, S.A., Grotzinger, J.P., Condon, J., Ramezani, J., Newall, M.J., and Allen, P.A., 2007,
161 Geochronologic constraints of the chronostratigraphic framework of the Neoproterozoic Huqf
162 Supergroup, Sultanate of Oman: American Journal of Science, v. 307, p. 1097-1145.

163 Butterfield, N.J., 2009, Oxygen, animals and oceanic ventilation: an alternative view: Geobiology,
164 v. 7, p. 1-7.

165 Calver, C.R., Black, L.P., Everard, J.L., and Seymour, D.B., 2004, U-Pb zircon age constraints on
166 late Neoproterozoic glaciation in Tasmania: Geology, v. 32, p. 893-896.

167 Condon, D.J., Schoene, B., McLean, N.M., Bowring, S.A., and Parrish, R.R., 2015, Metrology and
168 traceability of U-Pb isotope dilution geochronology (EARTHTIME Tracer Calibration Part I):
169 Geochimica et Cosmochimica Acta, v. 164, p. 464-480,

170 Condon, D., Zhu, M., Bowring, S., Wang, W., Yang, A., and Jin, Y., 2005, U-Pb ages from the
171 Neoproterozoic Doushantuo formation, China: Science, v. 308, p. 95-98.

172 Cox, G.M., Strauss, J.V., Halverson, G.P., Schmitz, M.D., McClelland, W.C., Stevenson, R.S., and
173 Macdonald, F.A., 2015, Kikiktat volcanics of Arctic Alaska – melting of harzburgitic mantle
174 associated with the Franklin large igneous province: Lithosphere L435-1. DOI:
175 10.1130/L435.1.

176 Domack, E.W., and Hoffman, P.F., 2011, An ice grounding-line wedge from the Ghaub glaciation
177 (635 Ma) on the distal foreslope of the Otavi carbonate platform, Namibia, and its bearing on
178 the snowball Earth hypothesis: Geological Society of America Bulletin, v. 123, p. 1448-1477.

179 Fairchild, I.J., and Kennedy, M.J., 2007, Neoproterozoic glaciation in the Earth System: Journal of
180 the Geological Society, v. 164, p. 895-921.

181 Halverson, G.P., Hoffman, P.F., Schrag, D.P., Maloof, A.C., and Rice, A.H.N., 2005, Toward a
182 Neoproterozoic composite carbon-isotope record: Geological Society of America Bulletin, v.
183 117, p. 1181-1207.

184 Hoffman, P.F., 2011, Strange bedfellows: glacial diamictite and cap carbonate from the Marinoan
185 (635 Ma) glaciation in Namibia: Sedimentology, v. 58, p. 57-119.

186 Hoffman, P.F., and Halverson, G.P., 2008, Otavi Group of the western Northern Platform, the
187 eastern Kaoko Zone and the Northern Margin Zone, *in* Miller, R.McG., ed., The Geology of
188 Namibia: Volume 2 Neoproterozoic to Lower Palaeozoic: Ministry of Mines and Energy,
189 Namibia, p. 13-69–13-136.

190 Hoffman, P.F., Hawkins, D.P., Isachsen, C.E., and Bowring, S.A., 1996, Precise U-Pb zircon ages
191 for early Damaran magmatism in the Summas Mountains and Weltwischia Inlier, northern
192 Damara Belt, Namibia. Communications of the Geological Survey of Namibia 11, 47-52.

193 Hoffman, P.F., Kaufman, A.J., Halverson, G.P., and Schrag, D.P., 1998, A Neoproterozoic
194 snowball Earth: Science, v. 281, p. 1342-1346.

195 Hoffman, P.F., and Schrag, D.P., 2002, The snowball Earth hypothesis: testing the limits of global
196 change: Terra Nova, v. 14, p. 129-155.

197 Hoffmann, K.H., Condon, D., Bowring, S., and Crowley, J., 2004, U-Pb zircon date from the
198 Neoproterozoic Ghaub Formation, Namibia: constraints on Marinoan glaciation: Geology, v.
199 32, p. 817-821.

200 Hoffmann, K.H., and Prave, A.R., 1996, A preliminary note on a revised subdivision and regional
201 correlation of the Otavi Group based on glacial diamictites and associated cap dolostones:
202 Communications of the Geological Survey of Namibia, v. 11, p. 77-82.

203 Jaffey, A.H., Flynn, K.F., Glendenin, L.E., Bentley, W.C., and Essling, A.M., 1971, Precision
204 measurement of half-lives and specific of ^{235}U and ^{238}U : Physics Reviews C4, p. 1889-1906.

205 Kasemann, S.A., Hawkesworth, C.J., Prave, A.R., Fallick, A.E., and Pearson, P.N., 2005, Boron
206 and calcium isotope composition in Neoproterozoic carbonate rocks from Namibia: evidence
207 for extreme environmental change: *Earth and Planetary Science Letters*, v. 231, p. 73-86.

208 Kennedy, M.J., Christie-Blick, N., and Prave, A.R., 2001, Carbon isotopic composition of
209 Neoproterozoic glacial carbonates as a test of paleoceanographic models for snowball Earth
210 phenomena: *Geology*, v. 29, p. 1135-1138.

211 Le Heron, D.P, Cox, G., Trundley, A., and Collins, A.S., 2011, Two Cryogenian glacial successions
212 compared: Aspects of the Sturt and Elatina sediment records of South Australia: *Precambrian
213 Research*, v. 186, p. 147-168.

214 Macdonald, F.A., Schmitz, M.D., Crowley, J.L., Roots, C.F., Jones, D.S., Maloof, A.C., Strauss,
215 J.V., Cohen, P.A., Johnston, D.T., and Schrag, D.P. 2010, Calibrating the Cryogenian:
216 *Science*, v. 327, p. 1241-1243.

217 Mattinson, J.M., 2005, Zircon U-Pb chemical abrasion ("CA-TIMS") method: Combined annealing
218 and multi-step partial dissolution analysis for improved precision and accuracy of zircon ages:
219 *Chemical Geology*, v. 220, p. 47-66.

220 Mattinson, J.M., 2010, Analysis of the relative decay constants of ^{235}U and ^{238}U by multi-step CA
221 TIMS measurements of closed-system natural zircon samples: *Chemical Geology*, v. 275, p.
222 186-198.

223 McLean, N., Condon, D.J., Schoene, B., and Bowring, S.A., 2015, Evaluating Uncertainties in the
224 Calibration of Isotopic Reference Materials and Multi-Element Isotopic Tracers
225 (EARTHTIME Tracer Calibration Part II): *Geochimica et Cosmochimica Acta*, v. 164, p.
226 481-501.

227 Miller, R. McG., 2008, *The Geology of Namibia: Neoproterozoic to lower Palaeozoic*. Ministry of
228 Mines and Energy, Geological Survey, Namibia.

229 Noble, S.R., Condon, D.J., Carney, J.N., Wilby, P.R., Pharoah, T.C., and Ford, T.D., 2015, U-Pb
230 geochronology and global context of the Charnian Supergroup, UK: Constraints on age of key
231 Ediacaran fossil assemblages. *Geological Society of America Bulletin*, v. 127, p. 250-265.

232 Och, L.M. & Shields-Zhou, G.A., 2012, The Neoproterozoic oxygenation event: Environmental
233 perturbations and biogeochemical cycling: *Earth-Science Reviews*, v. 110, p. 26-57.

234 Rooney, A.D., Macdonald, F.A., Strauss, J.V., Dudás, F.Ö., Hallmann, C., and Selby, D., 2014, Re-
235 Os geochronology and coupled Os-Sr isotope constraints on the Sturtian snowball Earth:
236 *Proceedings of the National Academy of Sciences*, v. 111, p. 51-56.

237 Rooney, A.D., Strauss, J.V., Brandon, A.D., and Macdonald, F.A., 2015, A Cryogenian
238 chronology: Two long-lasting synchronous Neoproterozoic glaciations: *Geology*, v. 43, p.
239 459-462.

240 Spence, G.H., Le Heron, D.P., and Fairchild, I.J., 2016, Sedimentological perspectives on climatic,
241 atmospheric and environmental change in the Neoproterozoic Era: *Sedimentology*, v. 63, p.
242 253-306.

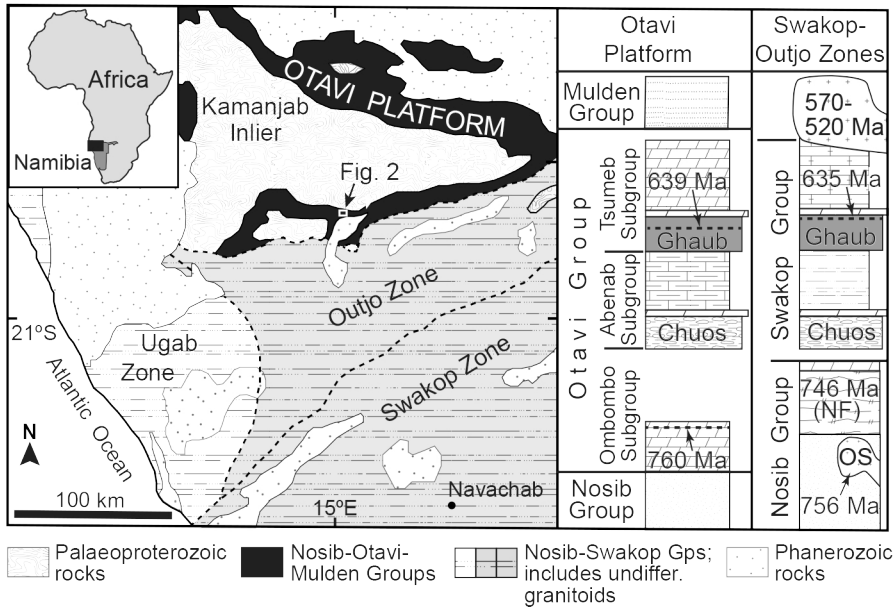
243 Sperling, E.A., Halverson, G.P., Knoll, A.H., Macdonald, F.A., and Johnston, D.T., 2013, A basin
244 redox transect at the dawn of animal life: *Earth and Planetary Science Letters*, v. 371-372, p.
245 143-155.

246 Zhang, S., Jiang, G., and Han, Y. 2008, The age of the Nantuo Formation and Nantuo glaciation in
247 South China: *Terra Nova*, v. 20, p. 289-294.

248 Zhou, C., Tucker, R., Xiao, S., Peng, Z. Yuan, X. and Chen, Z., 2004, New constraints on the ages
249 of Neoproterozoic glaciations in south China: *Geology*, v. 32, p. 437-440.

250

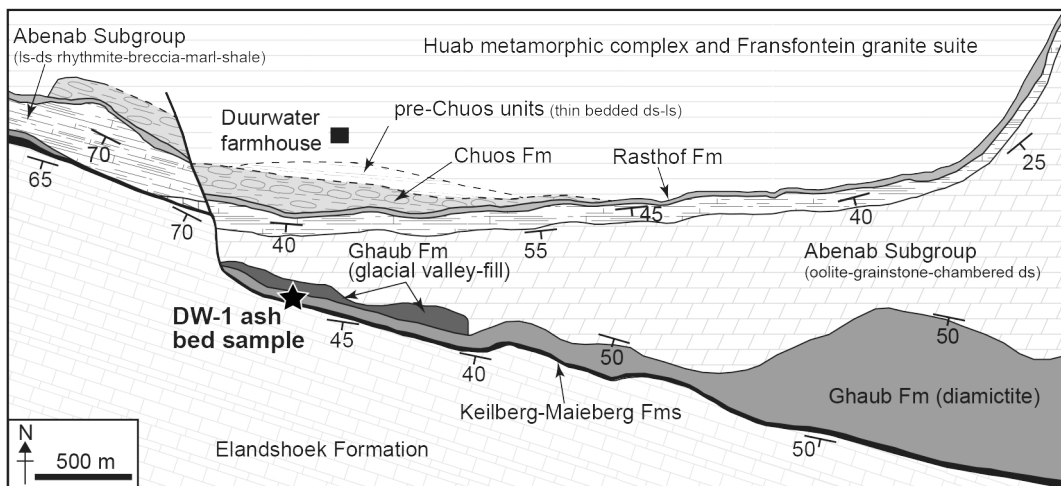
251 **Figure 1.** Generalised geologic framework of northern Namibia. Ages for the Naauwpoort
 252 Formation (NF) and Oas Syenite (OS) are from Hoffman et al. (1996), for the Ombombo Subgroup
 253 from Halverson et al. (2005), and for the Ghaub Formation from Hoffmann et al. (2004) and this
 254 paper. See Miller (2008, and references therein) for the ages of the granites that post-date the
 255 Swakop Group rocks.



256

257

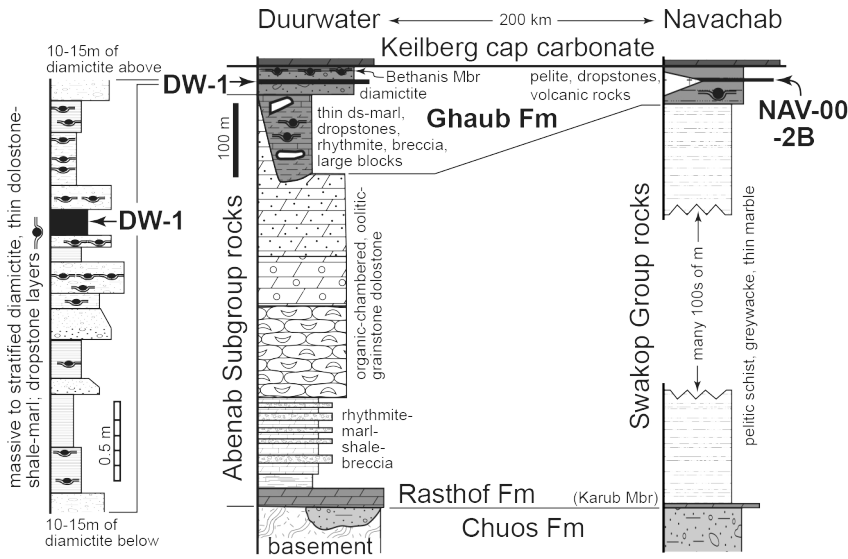
258 **Figure 2. A.** Fransfontein Ridge geology in the vicinity of sample DW-1. See Figure 1 for location.



259

260

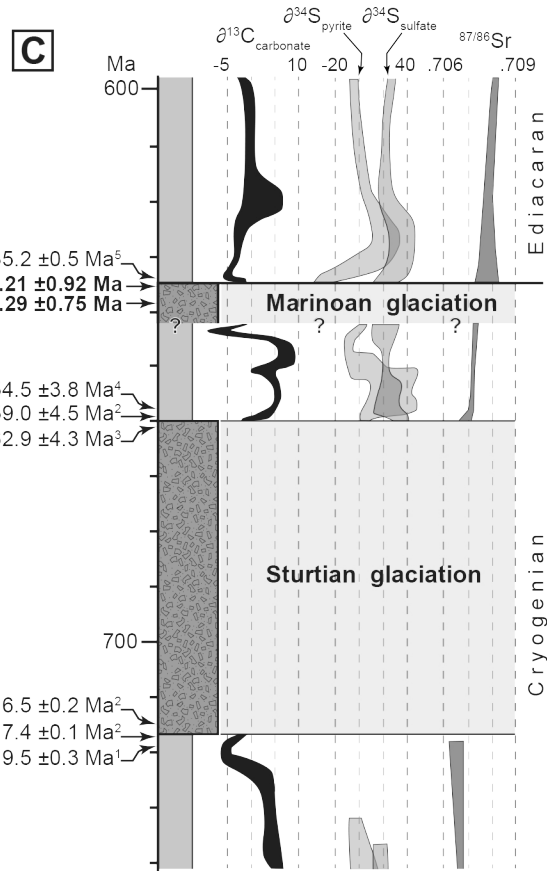
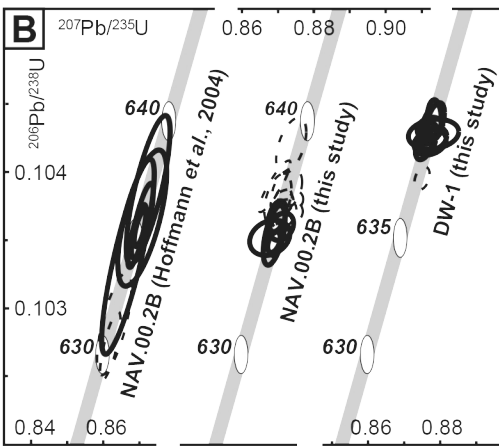
261 **Figure 3.** Simplified stratigraphy of the Duurwater and Navachab sections (for details of the
 262 Navachab section see Hoffmann et al., 2004); left column is a detailed section showing the
 263 stratigraphic position of the DW-1 ash bed within the diamictic interval of the Ghaub Formation.



264

265

266 **Figure 4. A.** DW-1 ash bed between ice-rafted-debris beds, Duurwater section. **B.** U-Pb Concordia
 267 plot of data for samples DW-1 and NAV-00-2B; solid ellipses represent analyses included in age
 268 calculation, dashed ellipses are not included (see Data Repository for explanation). **C.**
 269 Neoproterozoic timeline trends for key isotope proxy datasets: S isotopes after (from Och and
 270 Shields-Zhou, 2012, and references therein); Sr and C isotopes after (Halverson et al., 2005) and
 271 our own data. U-Pb age data from: 1–Cox et al. (2015), 2–Macdonald et al. (2010), 3–Zhou et al.
 272 (2004), 4–Zhang et al. (2008), 5–Condon et al. (2005). Bold ages are reported herein.



273